

Gas-cooling by dust during dynamical fragmentation

A. P. Whitworth^{*}, H. M. J. Boffin[†] and N. Francis[‡]

Department of Physics & Astronomy, University of Wales, Cardiff, CF2 3YB

28 February 2018

ABSTRACT

We suggest that the abrupt switch, from hierarchical clustering on scales $\gtrsim 0.04$ pc, to binary (and occasionally higher multiple) systems on smaller scales, which Larson has deduced from his analysis of the grouping of pre–Main-Sequence stars in Taurus, arises because pre-protostellar gas becomes thermally coupled to dust at sufficiently high densities. The resulting change from gas-cooling by molecular lines at low densities to gas-cooling by dust at high densities enables the matter to radiate much more efficiently, and hence to undergo dynamical fragmentation.

We derive the domain where gas-cooling by dust facilitates dynamical fragmentation. Low-mass ($\sim M_{\odot}$) clumps – those supported mainly by thermal pressure – can probably access this domain spontaneously, albeit rather quasistatically, provided they exist in a region where external perturbations are few and far between. More massive clumps probably require an impulsive external perturbation, for instance a supersonic collision with another clump, in order for the gas to reach sufficiently high density to couple thermally to the dust. Impulsive external perturbations should promote fragmentation, by generating highly non-linear substructures which can then be amplified by gravity during the subsequent collapse.

Key words: ISM: clouds - dust processes - Stars: formation

1 INTRODUCTION

Dynamical fragmentation (i.e. the growth of substructure during near-freefall collapse) is widely believed to play an important role in star formation, both as a means of forming star clusters, and as a means of forming binary systems (e.g. Bate, Bonnell & Price 1995; Bodenheimer, 1978; Bodenheimer & Boss, 1981; Bonnell & Bastian 1993; Bonnell & Bate 1994; Boss, 1991, 1993; Boss & Bodenheimer 1979; Burkert & Bodenheimer 1996; Chapman et al., 1992; Hoyle, 1953; Larson, 1972; Miyama, 1992; Miyama, Hayashi & Narita, 1984; Monaghan, 1994; Monaghan & Lattanzio, 1991; Myhill & Kaula, 1992; Nelson & Papaloizou, 1993; Pringle, 1989; Sigalotti & Klapp, 1994; Turner et al., 1995; Whitworth et al., 1995).

Recently Larson (1995) has analyzed the grouping of pre–Main-Sequence (pre-MS) stars in Taurus, and identified a critical length-scale $L_{\text{crit}} \sim 0.04$ pc. On larger scales the pre-MS stars appear to be clustered in a self-similar hierarchy, with the mean surface-density of neighbours N decreasing with angular separation θ as $N \propto \theta^{-0.62}$. On smaller scales the pre-MS stars have on average just one companion, which is usually tightly bound in a binary system; here the mean surface density of companions decreases as $N \propto \theta^{-2.15}$. Larson suggests that these binary (and

occasionally higher multiple) systems are formed by dynamical fragmentation. He proposes that L_{crit} is simply the Jeans length appropriate for the conditions prevailing in Taurus, and that the corresponding Jeans mass is $\sim M_{\odot}$. He then points out that if there is a preponderance of marginally Jeans-unstable clumps with $M \sim M_{\odot}$ collapsing and fragmenting into binary and triple systems, this will yield protostellar masses in the range 0.3 to 0.5 M_{\odot} , i.e. very close to the characteristic mass of the Initial Mass Function, $\sim 0.4M_{\odot}$.

However, there is a large range of densities in Taurus, and presumably an even large range of conditions in the various star-formation regions which form the entire ensemble of stars defining the Initial Mass Function. Therefore there must be a wide range of Jeans lengths.

Here we argue that the onset of fragmentation at the scale L_{crit} is in fact due to the density becoming just high enough for the gas to couple thermally with the dust, and thereby greatly increase its cooling efficiency, by availing itself of the dust’s continuum opacity. This circumstance defines a length-scale $\sim L_{\text{crit}}$ and a mass-scale $\sim M_{\odot}$ which are only weakly dependent on metallicity and environmental factors.

We concur with Larson’s inference that dynamical fragmentation will then tend to deliver protostars with masses around the peak in the IMF at $0.4M_{\odot}$.

Dynamical fragmentation can only occur if the gas cools efficiently by radiating. Specifically, the gas must be able to radiate away – on a dynamical timescale or faster – the internal energy gen-

^{*} e-mail: a.whitworth@astro.cf.ac.uk

[†] e-mail: h.boffin@astro.cf.ac.uk

[‡] e-mail: n.francis@astro.cf.ac.uk

erated by gravitational compression (Hoyle 1953, Rees 1976, Low & Lynden-Bell 1976, Silk 1977). At high densities this requires continuum opacity, and for cold ($T \lesssim 10^2$ K, say) gas having finite metallicity this opacity is supplied by dust.

Recently, Larson's analysis of the grouping of pre-MS stars in Taurus has been confirmed by Simon (1997). Simon has also repeated this analysis for the ρ Ophiuchus and Orion-Trapezium star-formation regions. He finds that the surface-densities of neighbours and companions obey similar power laws, $N \propto \theta^{-0.5 \pm 0.2}$ on large scales, and $N \propto \theta^{-2.0 \pm 0.1}$ on small scales. However, he finds that the switch occurs at different projected separations: ~ 0.06 pc in Taurus, ~ 0.025 pc in ρ Ophiuchus, and ~ 0.002 pc in Orion-Trapezium.

Simon argues that this variation is difficult to attribute to systematic changes in the Jeans length between the different star-formation regions. We propose that some of this variation arises because the different star-formation regions have very different large-scale surface densities. Proceeding from Taurus, through ρ Ophiuchus, to Orion-Trapezium, the large-scale surface-density of stars increases significantly, and so the switch must shift to smaller projected separations, even if the intrinsic distribution of binary separations is identical.

Kitsionas, Gladwin and Whitworth (1998) have also re-analyzed Taurus, with a larger sample of pre-MS stars. They have repeated this analysis for the Chamaeleon I star-formation region. Power-law fits to $N(\theta)$ give exponents similar to those obtained by Larson (1995) and Simon (1997). For Chamaeleon I the switch is at ~ 0.03 pc, as would be expected on the basis of its high overall surface-density.

In Section 2 and Appendix A we derive an expression for the compressional heating rate, $\mathcal{H}_{\text{comp}}$, in a recently formed fragment. In Section 3 we evaluate thermal coupling between gas and dust. In Section 4 and Appendix B we derive an expression for the cooling rate, $\mathcal{L}_{\text{dust}}$, due to thermal emission from dust. Appendix C demonstrates that for fragments having radius $R \lesssim 0.1$ pc, gas-cooling by dust dominates over gas-cooling by lines. In Section 5 we derive an expression for the mean (frequency-averaged) optical depth due to dust. In Section 6 we combine the results from the previous sections to define the domains on the (R, M) and (ρ, T) planes where gas-cooling by dust facilitates dynamical fragmentation. In Section 7 we discuss the results, and in Section 8 we summarize our main conclusions.

2 COMPRESSIONAL HEATING

For an approximately spherical fragment which has just become Jeans unstable, the mass M_j , radius R_j , temperature T and mean gas-particle mass \bar{m} are related by

$$\frac{G M_j}{R_j} = \frac{\mathcal{J} k T}{\bar{m}} \equiv \mathcal{J} a_o^2, \quad (1)$$

where \mathcal{J} is a numerical factor of order unity (see below), k is Boltzmann's constant, and $a_o = [kT/\bar{m}]^{1/2}$ is the isothermal sound speed.

If the gas remains isothermal, then by the time this fragment has contracted sufficiently for sub-fragments of mass SM_j to become Jeans unstable, the original fragment has radius $R = S^{2/3} R_j$, and is collapsing at speed $dR/dt = -\mathcal{M}(S)a_o$. Consequently the compressional heating rate is

$$\mathcal{H}_{\text{comp}} = -P \frac{dV}{dt} = 3M_j a_o^2 \frac{d \ln[R]}{dt}$$

$$= \left\{ \frac{\mathcal{J} \mathcal{M}(S)}{S^{2/3}} \right\} \frac{3 a_o^5}{G}. \quad (2)$$

In Appendix A we develop a simple time-dependent model of Jeans instability which enables us to estimate \mathcal{J} ($\simeq 2.36$), and $\mathcal{M}(S)$. For the purpose of numerical estimates, we set $S = 0.2$ (up to 5 fragments).

For completeness, we also include a cosmic-ray heating rate

$$\mathcal{H}_{\text{CR}} = \Gamma_o M, \quad (3)$$

with $\Gamma_o \simeq 2 \times 10^{-4}$ erg s $^{-1}$ g $^{-1}$. This corresponds to a cosmic-ray ionization rate $\mathcal{I}_{\text{CR}} \simeq 6 \times 10^{-17}$ s $^{-1}$. Eqn. (3) makes no allowance for the attenuation of cosmic rays in the interior of a dense fragment. However, this can only reduce the cosmic-ray heating rate, and it turns out that even the unattenuated rate is not very important in the regime with which we are concerned, i.e. the regime where gas-cooling by dust facilitates dynamical fragmentation.

3 THERMAL COUPLING BETWEEN GAS AND DUST

If the gas in a fragment is thermally coupled to the dust, the continuum opacity of the dust affords the fragment an efficient means of radiating away the internal energy generated by gravitational compression. Here we formulate the rate \mathcal{C} at which the gas transfers thermal energy to the dust.

If a fraction Z_{dust} by mass of the interstellar medium is in the form of spherical dust grains having radius r_{dust} and internal density ρ_{dust} , the rate of transfer of thermal energy to the dust is given by

$$\mathcal{C}_{\text{g-d}} = \frac{M}{\bar{m}} \left(\frac{8kT}{\pi \bar{m}} \right)^{1/2} \frac{3\rho Z_{\text{dust}}}{4r_{\text{dust}} \rho_{\text{dust}}} \times \left\{ 1 - \exp \left[\frac{-75\text{K}}{T} \right] \right\} \frac{k(T - T_{\text{dust}})}{(\gamma - 1)}. \quad (4)$$

For the purpose of numerical estimates we put $r_{\text{dust}} = 10^{-5}$ cm and $\rho_{\text{dust}} = 3$ g cm $^{-3}$. The term in braces, $\{ \}$, represents the accommodation coefficient, i.e. the mean inelasticity of collisions between gas particles and dust grains (Hollenbach & McKee 1979). For the low temperatures ($T \lesssim 100$ K) with which we are mainly concerned here, $\gamma \simeq 5/3$, since the rotational degrees of freedom of H $_2$ are not excited.

4 RADIATIVE COOLING

The maximum radiative cooling rate is obtained by assuming that the fragment radiates like a blackbody, i.e.

$$\mathcal{L}_{\text{BB}} = 4\pi R^2 \sigma_{\text{SB}} T^4. \quad (5)$$

This is a maximum cooling rate on four counts.

First, it assumes that the collapsing fragment exists in isolation. In reality, part of the luminosity from the fragment will be cancelled by the flux of background radiation incident on the surface of the fragment. The background radiation field will consist of a cosmic component at $T_o \sim 3$ K, plus a contribution from local sources such as stars, protostars, circumstellar cocoons and discs, warm molecular clouds. A detailed evaluation of this contribution would be extremely model-dependent. For the purpose of this paper, we represent the background with a single blackbody component at temperature $T_o \gtrsim 3$ K.

Second, it assumes that the cloud has continuum opacity at all wavelengths – or, at the very least, across a broad range of wavelengths near the peak of the blackbody spectrum.

Third, it assumes that, at these wavelengths around the peak, scattering is negligible compared with absorption and emission.

Fourth, it assumes that, at these wavelengths around the peak, the cloud is neither optically thin, nor very optically thick.

If we define a mean optical depth $\bar{\tau}(T)$ between the centre and the surface of the fragment (i.e. an optical depth averaged over the frequencies which contribute to radiative cooling of the fragment at temperature T), the radiative cooling rate is given approximately by

$$\mathcal{L}_{\text{rad}} \simeq 4\pi R^2 \sigma_{\text{SB}} \left\{ \frac{T^4 \bar{\tau}(T) \tau_{\text{crit}}}{(\bar{\tau}(T) + 1)(\bar{\tau}(T) + \tau_{\text{crit}})} - \frac{T_o^4 \bar{\tau}(T_o) \tau_{\text{crit}}}{(\bar{\tau}(T_o) + 1)(\bar{\tau}(T_o) + \tau_{\text{crit}})} \right\}. \quad (6)$$

Here, τ_{crit} is a critical optical depth, typically ~ 20 , and the second term in braces simply ensures that the cloud must be hotter than the background to cool radiatively. Eqn. (6) is constructed so as to give the correct asymptotic forms. For example, if $T_o = 0$, then in the optically thin limit,

$$\mathcal{L}_{\text{rad}} \longrightarrow 4\pi R^2 \sigma_{\text{SB}} T^4 \bar{\tau}(T) \quad (\bar{\tau}(T) < 1);$$

at modest optical depths,

$$\mathcal{L}_{\text{rad}} \longrightarrow 4\pi R^2 \sigma_{\text{SB}} T^4 \quad (1 < \bar{\tau}(T) < \tau_{\text{crit}});$$

and at high optical depths,

$$\mathcal{L}_{\text{rad}} \longrightarrow 4\pi R^2 \sigma_{\text{SB}} \frac{\tau_{\text{crit}}}{\bar{\tau}(T)} \quad (\bar{\tau}(T) > \tau_{\text{crit}}).$$

This last form is derived in Appendix B, and takes account of the fact that high luminosities can only be transported through the interior of an optically thick fragment if there is a sufficiently large temperature difference between the centre of the fragment and its surface. To take account of this, we require that no more than a fraction f of the fragment's mass be hotter than FT , where T is now specifically the surface temperature. Hence the precise value of τ_{crit} depends on our choice of f and F , and also on β (the emissivity index): $\tau_{\text{crit}} = \tau_{\text{crit}}(f, F, \beta)$. Substituting $f = 1/3$, $F = 2$ (i.e. at least 2/3 of the fragment is below $2T$), we obtain $\tau_{\text{crit}} = 47.9$ & 30.8 for $\beta = 1$ & 2 respectively (see Appendix B). For the purpose of numerical estimates we shall adopt $\beta = 1.5$ and $\bar{\tau}_{\text{crit}} = 38.3$.

5 DUST OPACITY

The mean dust optical depth between the centre and the surface of a spherical, uniform-density fragment is

$$\bar{\tau}(T_{\text{dust}}) = \frac{9MZ_{\text{dust}}\bar{Q}(T_{\text{dust}})}{16\pi R^2 r_{\text{dust}} \rho_{\text{dust}}},$$

where $\bar{Q}(T_{\text{dust}})$ is the Planck-mean absorption efficiency of a dust grain. Since our main concern here is with long wavelength radiation from dust at low temperatures, we adopt the prescription

$$\bar{Q}(T_{\text{dust}}) = 0.0004 \left[\frac{T_{\text{dust}}}{10\text{K}} \right]^\beta, \quad 1 \lesssim \beta \lesssim 2.$$

This corresponds to a mean mass-opacity coefficient $\bar{\kappa}(T_{\text{dust}}) = 3Z_{\text{dust}}\bar{Q}(T_{\text{dust}})/4r_{\text{dust}}\rho_{\text{dust}} \simeq 10\text{ cm}^2\text{ g}^{-1} Z_{\text{dust}} [T_{\text{dust}}/10\text{K}]^\beta$, and hence a mean optical depth

$$\bar{\tau}(T_{\text{dust}}) \simeq 2.4\text{ cm}^2\text{ g}^{-1} Z_{\text{dust}} \frac{M}{R^2} \left[\frac{T_{\text{dust}}}{10\text{K}} \right]^\beta \quad (7)$$

(cf. Hildebrand (1983), who recommends $Q(\lambda = 250\mu\text{m}) = 0.0004$ and $\kappa(\lambda = 250\mu\text{m}) = 0.1\text{ cm}^2\text{ g}^{-1}$).

To account for dust evaporation, we multiply Eqn. (7) by a factor

$$1 - 0.4 \exp\left[-\frac{100\text{K}}{T_{\text{dust}}}\right] - 0.6 \exp\left[-\frac{1000\text{K}}{T_{\text{dust}}}\right].$$

The second term represents evaporation of the volatile grain mantle at temperatures of order 100 K, and the third term represents evaporation of the refractory core at temperatures of order 1000 K. This rather *ad hoc* prescription is adequate for our purposes, since we are mainly concerned with gas-cooling by dust in the regime where the dust is cool and evaporation is negligible.

6 GAS-COOLING BY DUST DURING DYNAMICAL FRAGMENTATION

The domain in which gas-cooling by dust facilitates quasi-freefall collapse and dynamical fragmentation (hereafter the *dust-domain*) is given by[§]

$$\mathcal{H}_{\text{comp}} + \mathcal{H}_{\text{CR}} \lesssim \{C_{\text{g-d}}^{-1} + \mathcal{L}_{\text{rad}}^{-1}\}^{-1}. \quad (8)$$

The dust-domain can be defined on both the (R, M) and the (ρ, T) planes, using Eqn. (1) and $\rho = 3M/4\pi R^3$ to convert from one to the other.

In order to simplify the analysis, we put $T_{\text{dust}} = T_o = 10\text{ K}$ in $C_{\text{g-d}}$ (Eqn. (4)), and $T_{\text{dust}} = T$ in \mathcal{L}_{rad} (Eqn. (6)). To justify this we note that the section of the dust-domain boundary where $C_{\text{g-d}}$ is important is quite distinct from the section where \mathcal{L}_{rad} is important, *viz.*

Consider first the large- R limit of the dust-domain, where $C_{\text{g-d}} \ll \mathcal{L}_{\text{rad}}$, so $C_{\text{g-d}}$ dominates the righthand side of Inequality (8), i.e. the critical process is the transfer of thermal energy from the gas to the dust. Under this circumstance the thermal balance of the dust involves a much more rapid energy turnover than that of the gas (e.g. Whitworth & Clarke 1997). Hence the heat input from thermal coupling to the gas makes a negligible contribution to the thermal balance of the dust. The dust temperature T_{dust} is determined by the background radiation field, and adopts a value of order the background temperature T_o .

Next consider the small- R limit of the dust-domain, where $C_{\text{g-d}} \gg \mathcal{L}_{\text{rad}}$, so \mathcal{L}_{rad} dominates the righthand side of Inequality (8), i.e. the critical process is the emission of radiation by the dust and its escape from the fragment. At these high densities the gas and dust are closely coupled. A very small temperature difference suffices to transfer the compressional heating of the gas to the dust, and we can approximate $T_{\text{dust}} \simeq T$.

In between these two limits, the dust-domain boundary is determined at high temperatures by dust evaporation, and at low temperatures by the fact that the gas cannot cool below the background temperature. Consequently there is no need to formulate accurately the circumstances under which $C_{\text{g-d}} \sim \mathcal{L}_{\text{rad}}$.

Figure 1 shows contours of constant

$$\mathcal{R} \equiv (\mathcal{H}_{\text{comp}} + \mathcal{H}_{\text{CR}}) (C_{\text{g-d}}^{-1} + \mathcal{L}_{\text{rad}}^{-1})$$

[§] The two heating processes operate simultaneously, and so their rates add in parallel. The two cooling processes operate sequentially, and so their rates add in series.

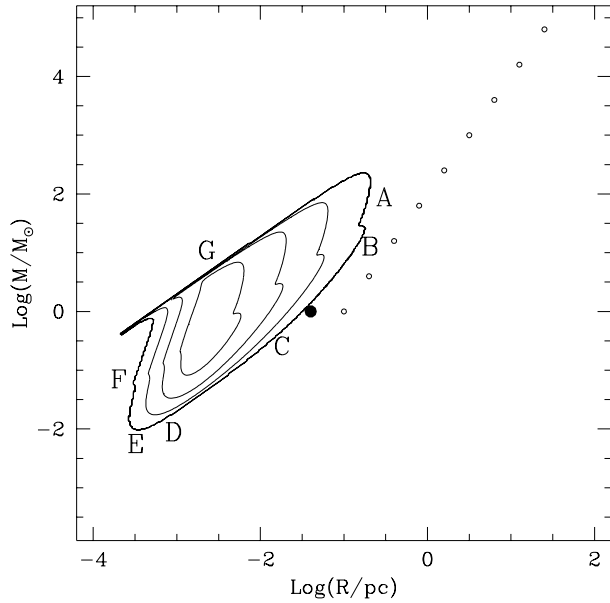


Figure 1. The (R, M) plane. The outer contour is the limit of the dust-domain, where gas-cooling by dust enables the gas to fragment dynamically. The other contours show where the ratio of compressional heating to gas-cooling by dust equals 0.32, 0.10 & 0.03. The letters refer to the different processes limiting the dust-domain, as discussed in the text. The line of open circles represents the average observed properties of clumps. The large dot marks the point $(0.04 \text{ pc}, M_{\odot})$, i.e. the critical entity identified by Larson.

on the (R, M) plane, for $\beta = 1.5$, $T_0 = 10\text{K}$, and $Z_{\text{dust}} = 0.01$. The region inside the outer contour is the dust-domain. Contours are drawn for $\mathcal{R} = 1.00, 0.32, 0.10$ & 0.03 , to emphasize how efficient gas-cooling by dust becomes inside the dust-domain.

Starting at the righthand side, and working round in a clockwise sense, the dust-domain limits are caused by (A) gas-dust coupling in the high-temperature (elastic) limit; (B) gas-dust coupling in the low-temperature (perfectly inelastic) limit; (C) the background temperature acting as a minimum temperature ($T \geq T_0$); (D) the dust being optically thin; (E) the dust optical depth being intermediate ($1 \lesssim \tau \lesssim \tau_{\text{crit}}$); (F) the dust being optically thick; (G) dust evaporation. *Partial* dust evaporation actually promotes fragmentation in the high density limit by reducing the dust optical depth, but it inhibits gas-dust coupling; this is why the dust-domain boundaries curve towards higher densities as they approach the evaporation limit. The same contours are presented on the (ρ, T) plane in Figure 2. The dashed line indicates the background temperature T_0 .

The most relevant part of the dust-domain is probably the part corresponding to low temperatures, $T \lesssim 50\text{K}$, but we have plotted the whole domain in order to avoid the extremely model-dependent complexities of predicting the gas temperature precisely.

Of course, to be important in this context gas-cooling by dust must not only be able to handle the net heating of a fragment, it must also be able to handle it more effectively than, or at least as effectively as, gas-cooling by lines. Figure 1 shows that the dust-domain has $R \lesssim 0.1\text{pc}$, and Appendix C demonstrates that for protostellar fragments with $R \lesssim 0.1\text{pc}$, gas-cooling by dust is more effective than gas-cooling by lines.

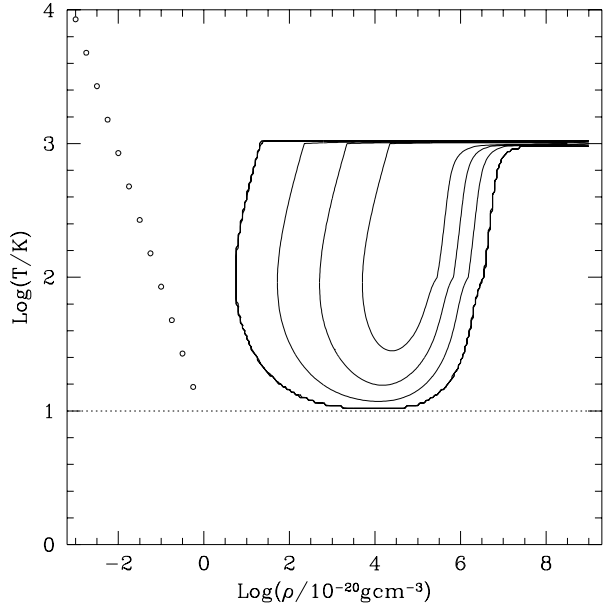


Figure 2. The (ρ, T) plane. The outer contour is the limit of the dust-domain, where gas-cooling by dust enables the gas to fragment dynamically. The other contours show where the ratio of compressional heating to gas-cooling by dust equals 0.32, 0.10 & 0.03. The line of open circles represents the average observed properties of clumps. The dashed line represents the background temperature.

7 DISCUSSION

On Figure 1, we have also plotted the mean observed distribution of clump masses and radii, as collated by Chièze (1987). This distribution approximates to

$$M \simeq M_{\odot} \left[\frac{R}{0.1\text{pc}} \right]^2.$$

and is marked by a line of open circles on Figure 1. If the clumps were thermally virialized, we could use Eqn. (1) to convert this distribution into

$$T \simeq 8.5 \text{ K} \left[\frac{\rho}{10^{-20} \text{ g cm}^{-3}} \right]^{-1};$$

and this is marked by the line of open circles on Figures 2.

However, all but the very low-mass clumps are supported by non-thermal motions, with the gas being at rather low temperatures, typically in the range 10 to 15 K, and seldom above 50K. Thus, although the locus of clumps in Figure 1 appears to run rather close to the boundary of the dust-domain, it is only the low-mass clumps – those supported mainly by thermal pressure – that are really close to the dust-domain. Even these may be unable to access the dust-domain without some external perturbation.

The gas in a high-mass clump can probably only enter the dust-domain if it is compressed and heated by a shock, for example following a collision with another clump of comparable mass, or as a consequence of being overrun by an expanding nebula (HII region, stellar-wind bubble or supernova remnant). Gas-cooling by lines will play an important role in such shocks (as a means of removing the dissipated energy), but Appendix C shows that the shock-compressed gas will then only be able to condense further and fragment if it is dense enough to couple thermally to the dust.

A number of observations might be explained on the basis of the dust-domain and its relation to the locus of observed clumps.

7.1 Low-mass clumps

Low-mass ($\sim M_{\odot}$) clumps are supported mainly by thermal pressure (Myers 1983). Therefore, in the absence of external perturbations, they should relax to hydrostatic equilibrium. However, Figures 1 & 2 suggest that such clumps need a relatively small external perturbation – and possibly no perturbation at all – to enter the dust-domain. Consequently we might expect a large fraction of stars to be formed from the collapse of such clumps. If dynamical fragmentation leads typically to the formation of a binary or triple system, with most of the clump mass ending up in the component stars, then the Initial Mass Function (IMF) should peak in the range 0.2 to $0.5 M_{\odot}$, as it apparently does (Scalo 1986). This last point was emphasized by Larson (1995).

Moreover, if an external perturbation is involved, this should greatly increase the chances of permanent fragmentation during the ensuing collapse. This is because the clump would be delivered into the dust-domain with highly non-linear substructure, and gravity would then rapidly amplify this non-linear substructure during the subsequent quasi-freefall collapse.

By contrast, if it is possible for a clump to condense quasistatically into the dust-domain, it arrives there in a rather too well organized state, and collapse seems likely to lead to a single star. Under this circumstance, binary formation may require some sort of intrinsic instability, for example in a circumstellar disc.

Support for the notion that even low-mass clumps either require an external perturbation to trigger their collapse, or condense rather quasistatically into the dust-domain before collapsing to form stars, comes from the observation (Myers, private communication) that the majority of starless low-mass clumps are located in the outer reaches of Taurus, where presumably external perturbations are few and far between.

Further support comes from the observation that in low-mass clumps associated with IRAS sources, the IRAS source (i.e. the putative newly-formed star) is normally significantly displaced from the centre of the (presumably placental) clump (Beichman et al. 1986, Clark 1987).

7.2 High-mass clumps

High-mass ($\gtrsim 10M_{\odot}$) clumps are supported mainly by non-thermal motions. From Figure 2, it appears that they are unable to enter the dust-domain, without a substantial external impulse – most likely a shock, due to a collision with another comparable clump, or due to being overrun by an expanding nebula. A sufficiently strong shock would compress the gas to the point where it became thermally coupled to the dust. If our hypothesis is correct, this would lead to efficient fragmentation and the formation of a star-cluster.

There is evidence that molecular clouds have an hierarchical structure, i.e. clumps nested within clumps. If this is so, a high-mass clump should be envisaged as an ensemble of lower-mass clumps. Consequently, even when star formation is triggered in a high-mass clump (by an external perturbation), most of the gas ending up in stars will probably reside in low-mass ($\sim M_{\odot}$) sub-clumps, and this should lead to a majority of the stars formed having masses in the range 0.2 to $0.5 M_{\odot}$.

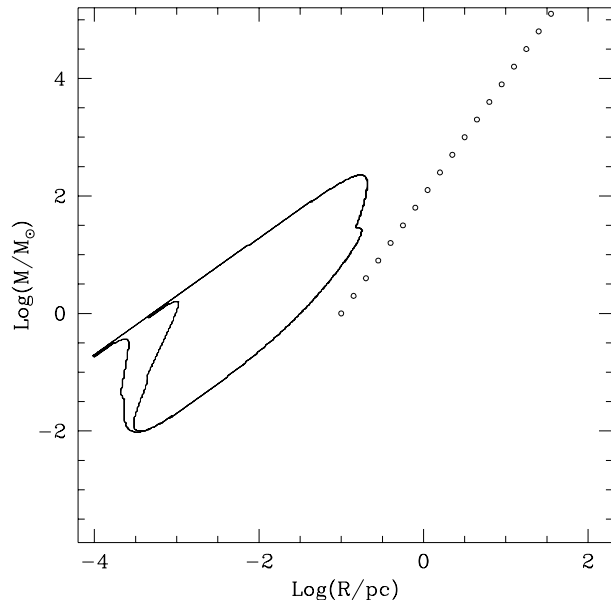


Figure 3. The (R, M) plane. The effect on the dust-domain of varying the far-infrared emissivity index β . The heavy contour delimits the dust-domain when $\beta = 1$. The light contour delimits the dust-domain when $\beta = 2$. Note that the two contours only diverge at small R .

7.3 M_{\min} and M_{\max}

Several authors (Rees 1976, Low & Lynden-Bell 1976, Silk 1977) have determined the minimum mass for star formation M_{\min} on the basis of opacity-limited fragmentation. With reference to Figure 1, this is equivalent to identifying M_{\min} with the smallest mass falling inside the dust-domain, and it yields a value $M_{\min} \sim 0.01M_{\odot}$. However, to reach this part of the dust-domain from the conditions obtaining inside a clump would require either (i) several consecutive fragmentation episodes, or (ii) a single fragmentation episode generating a very large number of pieces. Numerical simulations (Larson 1978) suggest that dynamical fragmentation is a one-stage process, i.e. that during freefall gravity only amplifies the substructure which is present at the outset. This implies that (i) cannot work, and that (ii) requires an external perturbation with improbably high power on high spatial frequencies. Therefore we do not expect many stars with masses $\sim 0.01M_{\odot}$.

The largest mass falling inside the dust-domain is $M_{\max} \sim 100M_{\odot}$. We speculate that this is because clumps having higher mass cannot (coherently) enter the dust-domain, no matter what external perturbation they experience, and therefore cannot collapse to form stars.

7.4 Dependence on β , T_o and Z_{dust}

In Figure 3 we show how the dust-domain is altered on the (R, M) plane, if one adopts a different far-infrared emissivity index for the dust, i.e. $\beta = 1$ or $\beta = 2$. The only significant change is on the small- R boundary of the dust-domain, where the dust is optically thick to its own radiation. Since we are here more concerned with the large- R boundary, this variation will not affect our conclusions significantly.

In Figure 4 we show how the dust-domain is altered on the (R, M) plane, if one adopts a different background temperature,

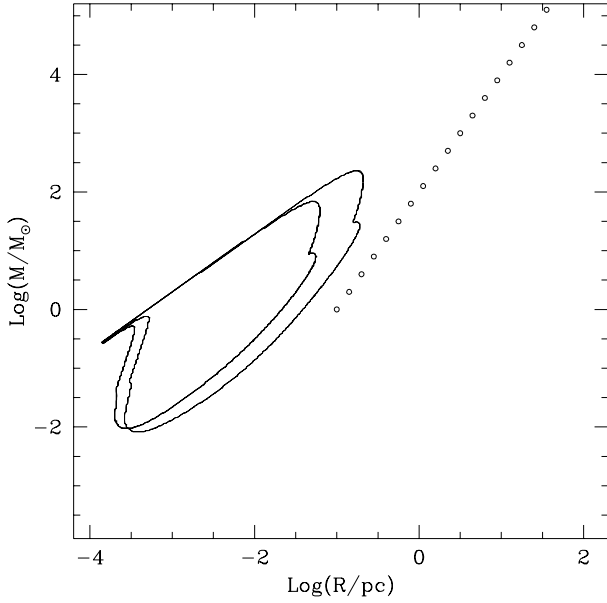


Figure 4. The (R, M) plane. The effect on the dust-domain of reducing the metallicity to $Z_{\text{dust}} = 0.003$, heavy contour; and reducing the background temperature to $T_0 = 5$ K, light contour.

i.e. $T_0 = 5$ K (instead of $T_0 = 10$ K), or a different metallicity, i.e. $Z_{\text{dust}} = 0.003$ (instead of $Z_{\text{dust}} = 0.01$). Changing the background temperature has little effect on the boundary of the dust-domain where it is close to the locus of clumps.

Reducing the metallicity moves the dust-domain to smaller R -values. Unless the locus of clumps is also different, in the sense of being characterized by a larger mean column-density, this increases the gap between the dust-domain and the locus of clumps. Consequently, where the metallicity is well below solar, it should be much harder for star formation to occur spontaneously. This might mean that star formation is more dependent on an external impulse, and hence that star formation is more likely to occur in bursts. This could dictate the pattern of star formation in a galaxy having low metallicity, for example a young galaxy or an irregular galaxy – in the sense of making star formation more burst-like.

8 CONCLUSIONS

We have evaluated the conditions under which gas-cooling by dust enables a clump to collapse and fragment dynamically. We describe these conditions as the *dust-domain*. We have also shown that in the dust-domain gas-cooling by dust dominates over gas-cooling by dust.

The observed properties of clumps in star-forming molecular clouds are such that low-mass ($\sim M_\odot$) clumps are close to the dust-domain. Consequently only a small external perturbation is needed to propel them into the dust-domain – and possibly no perturbation at all. Therefore, if such clumps fragment into binary or triple systems, with most of their mass ending up in the components of these systems, they will spawn stars having masses concentrated in the range 0.2 to 0.5 M_\odot , which is the peak of the IMF (cf. Larson 1995).

In isolated quiescent regions, low-mass cores may survive for long periods, for lack of a sufficient external impulse to trigger

(or accelerate) their collapse. They would be observed as starless clumps.

High-mass clumps require a substantial external impulse to reach the dust-domain and start collapsing. Collisions with other clumps and/or shocks due to expanding nebulae can provide a sufficient impulse. This may be why star formation is (apparently) more efficient in dynamically agitated regions.

The dust-domain may also define the minimum and maximum masses for star formation, $M_{\text{min}} \sim 0.01M_\odot$ and $M_{\text{max}} \sim 100M_\odot$, but the majority of stars should fall well within these limits.

In regions of low metallicity, for instance irregular galaxies, star formation may be more prone to occur in bursts.

Appendix A. Isothermal fragmentation

Consider a uniform medium with density ρ_0 and isothermal sound speed a_0 . Now suppose that a spherical fragment having radius R_0 , and hence mass $M_0 = 4\pi R_0^3 \rho_0 / 3$, attempts to condense out of the background by contracting homologously, so that it remains spherical with instantaneous radius R , and uniform with instantaneous density $\rho = \rho_0 (R/R_0)^3$. Further suppose that the isothermal sound speed is constant, $a = a_0$, and that the external medium exerts a constant pressure $P_{\text{ext}} = \rho_0 a_0^2$ at the boundary of the fragment. Radial excursions of the fragment are controlled by a potential function $\phi(R)$, in the sense that $d^2R/dt^2 = -d\phi/dR$ and $(dR/dt) = [-2\phi(R)]^{1/2}$. $\phi(R)$ is derived (Whitworth 1981) from the energy equation

$$\frac{d}{dt} \{ \mathcal{K} + \mathcal{G} \} = [P_{\text{int}} - P_{\text{ext}}] \frac{dV}{dt}, \quad (9)$$

where $\mathcal{K} = (3/10)M_0(dR/dt)^2$ is the radial kinetic energy, $\mathcal{G} = -3GM_0^2/5R$ is the self-gravitational potential energy, and $P_{\text{int}} = 3M_0 a_0^2 / 4\pi R^3$ is the internal pressure. $\phi(R)$ can be written in the form

$$\begin{aligned} \frac{\phi(R)}{a_0^2} = & -\frac{15}{2^{8/3}} \left(\frac{R_0}{R_1} \right)^2 \left[\left(\frac{R}{R_0} \right)^{-1} - 1 \right] \\ & - 5 \ln \left(\frac{R}{R_0} \right) + \frac{5}{3} \left[\left(\frac{R}{R_0} \right)^3 - 1 \right], \end{aligned} \quad (10)$$

where the first term on the righthand side represents self-gravity, the second term internal pressure, the third term external pressure, and

$$R_1 = \frac{3}{2^{7/3}} \left(\frac{5}{\pi G \rho_0} \right)^{1/2} a_0. \quad (11)$$

Stable equilibrium states ($d\phi/dR = 0$, $d^2\phi/dR^2 > 0$) exist only for $R_0 < R_1$; for $R_0 \geq R_1$ the fragment contracts indefinitely. Therefore R_1 can be identified as the Jeans radius. The Jeans mass is given by

$$M_1 = \frac{4\pi R_1^3 \rho_0}{3} = \frac{3^2 \pi}{2^5} \left(\frac{5}{\pi G} \right)^{3/2} \frac{a_0^3}{\rho_0^{1/2}}, \quad (12)$$

and so

$$\mathcal{J} \equiv \frac{G M_1}{R_1 a_0^2} = \frac{15}{2^{8/3}} \simeq 2.3623. \quad (13)$$

If we consider a marginally Jeans-unstable fragment with mass M_1 , starting to condense out from radius R_1 , then by the time sub-fragments with mass $\mathcal{S}M_1$ become Jeans unstable, the radius

of the initial fragment has decreased to $S^{2/3}R_i$. From Eqn. (10), it follows that the Mach Number of the contraction is given by

$$\mathcal{M}(S) \equiv -\frac{dR/dt}{a_o} = \left\{ \frac{15}{2^{5/3}} [S^{-2/3} - 1] + \frac{20}{3} \ln[S] + \frac{10}{3} [1 - S^2] \right\}^{1/2}. \quad (14)$$

Representative values of $\mathcal{M}(S)$ are tabulated below

S	\mathcal{M}	$\mathcal{M}/S^{2/3}$
0.5	0.81	1.41
0.4	0.82	1.51
0.3	0.91	2.03
0.2	1.25	3.65
0.1	2.27	10.54

The slow variation of \mathcal{M} with S for $S \sim 0.5$ reflects the fact that the point of inflexion ($d^2\phi/dR^2 = 0$) which defines the marginally Jeans-unstable fragment occurs at $S = 0.5$, $R = S^{2/3}R_i \simeq 0.63R_i$. Consequently acceleration of the collapse is slow at this stage.

There is apparently an inconsistency in the above analysis, in the sense that – strictly speaking – a marginally Jeans-unstable fragment would be centrally condensed, and hence the value of \mathcal{J} would be smaller than the one we have derived. However, since here we are mainly concerned with dynamical fragmentation, we do not envisage there being sufficient time for the fragment of the moment to relax towards detailed hydrostatic balance. Therefore it is appropriate to use the results we have derived on the basis of a uniform-density fragment.

Appendix B. Radiative transport inside an optically thick fragment

In order to estimate the temperature difference required to drive radiative energy transport from the centre of the fragment to its surface in the high optical depth limit, we introduce a dummy optical depth variable τ' with $\tau' = 0$ at the centre and $\tau' = \bar{\tau}(T)$ at the surface. For this calculation, we must allow that the temperature is a function of position $\theta(\tau')$, and increases from $\theta = T$ at the surface to higher values in the interior. We shall adopt the condition that isothermality breaks down once a fraction f of the fragment's mass is heated above FT , and adopt $f = 1/3$, $F = 2$.

Since the mean dust opacity depends on temperature (see Eq. (7)), the effective optical-depth differential is

$$(\theta/T)^\beta d\tau',$$

and so the flux is given by

$$F(\tau') \simeq -\frac{4}{3} \frac{d}{(\theta/T)^\beta d\tau'} [\sigma\theta^4(\tau')].$$

For simplicity we assume that heat is deposited uniformly throughout the fragment, so the divergence of the flux must satisfy

$$\begin{aligned} \nabla \cdot \mathbf{F} &\equiv \frac{1}{r^2} \frac{d}{dr} \{r^2 F(\tau)\} \\ &\equiv -\frac{16\sigma T^\beta \bar{\tau}(T)}{3R} \frac{1}{\tau'^2} \frac{d}{d\tau'} \left\{ \tau'^2 \theta^{(3-\beta)}(\tau') \frac{d\theta}{d\tau'} \right\} \\ &= \frac{3\mathcal{H}_{\text{comp}}}{4\pi R^3} \end{aligned} \quad (15)$$

where we have substituted $r = R\tau'/\bar{\tau}(T)$ and $dr = R d\tau'/\bar{\tau}(T)$.

Integrating this equation, and applying the boundary conditions $d\theta/d\tau' = 0$ at $\tau' = 0$, and $\theta = T$ at $\tau' = \bar{\tau}(T)$, we obtain

$$\begin{aligned} \theta^{(4-\beta)}(\tau') &= T^{(4-\beta)} \\ &+ \frac{3(4-\beta)\mathcal{H}_{\text{comp}}\bar{\tau}(T)}{128\pi R\sigma T^\beta} \left\{ 1 - \left[\frac{\tau'}{\bar{\tau}(T)} \right]^2 \right\}. \end{aligned} \quad (16)$$

Substituting $\tau'/\bar{\tau}(T) = f^{1/3}$ and $\theta(\tau') < FT$, gives the condition for approximate isothermality to break down:

$$\begin{aligned} \frac{\mathcal{H}_{\text{comp}}\bar{\tau}(T)}{4\pi R^2\sigma T^4} &< \tau_{\text{crit}}(f, F, \beta) \\ &= \frac{32 [F^{(4-\beta)} - 1]}{3 [4 - \beta] [1 - f^{2/3}]}. \end{aligned} \quad (17)$$

For $f = 1/3$ and $F = 2$, we obtain the values

β	=	1.00	1.50	2.00
τ_{crit}	\simeq	47.9	38.3	30.8

Appendix C. Gas-cooling by dust versus gas-cooling by lines

Consider a molecule with mass m_x and moment of inertia I_x . Its rotational energy levels are at $E_J = J(J+1)\hbar^2/2I_x \simeq J^2\hbar^2/2I_x$, and they will be significantly excited up to $E_{J_{\text{highest}}} = \mathcal{F}kT$ (where \mathcal{F} is a factor of order unity), so we can put

$$J_{\text{highest}} \simeq \frac{[2\mathcal{F}I_x kT]^{1/2}}{\hbar}.$$

The rotational lines have

$$h\nu_{(J \rightarrow J-1)} = \frac{J\hbar^2}{I_x} \longrightarrow \nu_{(J \rightarrow J-1)} = \frac{J\hbar}{2\pi I_x}$$

and hence

$$h\nu_{(J \rightarrow J-1)} \leq h\nu_{(J_{\text{highest}} \rightarrow J_{\text{highest}}-1)} \simeq \frac{2\mathcal{F}kT}{J_{\text{highest}}}.$$

To calculate the maximum possible cooling rate due to this molecule, we assume that all the lines up to and including ($J_{\text{highest}} \rightarrow J_{\text{highest}} - 1$) are optically thick.

Under this circumstance, the intensity in a line is given by the Planck Function. Again, since we are after a maximum possible cooling rate, we can replace the Planck Function with the Rayleigh-Jeans approximation, $B_\nu(T) \simeq 2kT\nu^2/c^2$. Since the peak of the Planck Function is at $h\nu \simeq 5kT$, whereas the highest frequency optically thick cooling line is at $h\nu_{(J_{\text{highest}} \rightarrow J_{\text{highest}}-1)} \simeq 2\mathcal{F}kT/J_{\text{highest}}$, this is actually a fairly good approximation as long as $J_{\text{highest}} > 0.4\mathcal{F}$.

The width of a line is determined by the velocity dispersion. For the thermally supported low-mass clumps with which we are concerned the velocity width is given by

$$\Delta v \sim 4 \left[\frac{2kT}{\pi m_x} \right]^{1/2} = 4a_o \left[\frac{2\bar{m}}{\pi m_x} \right]^{1/2}.$$

If we consider a clump of mass M and radius R , then the maximum cooling rate due to a single line from this particular molecule is

$$\mathcal{C}_J \simeq 4\pi R^2 \pi [B_\nu(T) - B_\nu(T_0)] \left. \frac{\nu \Delta v}{c} \right|_{\nu=J\hbar/2\pi I_X} \quad (18)$$

$$\simeq \frac{4R^2 k [T - T_0] a}{\pi} \left[\frac{2\bar{m}}{\pi m_X} \right]^{1/2} \left[\frac{\hbar J}{c I_X} \right]^3 \quad (19)$$

where T_0 is the temperature of the background radiation field.

The total cooling rate due to the molecule is obtained by summing over all the lines:

$$\mathcal{C}_X \simeq \sum_{J=1}^{J_{\text{highest}}} \{\mathcal{C}_J\} \quad (20)$$

$$\simeq \frac{R^2 k [T - T_0] a}{\pi} \left[\frac{2\bar{m}}{\pi m_X} \right]^{1/2} \left[\frac{\hbar}{c I_X} \right]^3 \frac{J_{\text{highest}}^4}{4} \quad (21)$$

$$\simeq \frac{4\mathcal{F}^2 R^2 \bar{m}^2 k [T - T_0] a^5}{\pi c^3 \hbar I_X} \left[\frac{2\bar{m}}{\pi m_X} \right]^{1/2} \quad (22)$$

From the results of Neufeld, Lepp & Melnick (1995), we infer that at high densities (*i.e.* in the optically thick limit) $^{12}\text{C}^{16}\text{O}$ contributes $\sim 4\%$ of the net cooling, so we put $m_X = m_{\text{CO}} \simeq 5 \times 10^{-23}$ g, $I_X = I_{\text{CO}} \simeq 6 \times 10^{-38}$ g cm² s⁻¹, and write the net cooling rate in the form

$$\begin{aligned} \mathcal{C}_{\text{line}} &\simeq \mathcal{N} \mathcal{C}_{\text{CO}} \\ &\simeq \frac{4\mathcal{N}\mathcal{F}^2 R^2 \bar{m}^2 k [T - T_0] a^5}{\pi c^3 \hbar I_{\text{CO}}} \left[\frac{2\bar{m}}{\pi m_{\text{CO}}} \right]^{1/2} \end{aligned} \quad (23)$$

where $\mathcal{N} \simeq 25$ is intended to represent the contribution from 24 other similar molecular lines from different molecules and/or isotopic variants. This net gas-cooling rate due to (molecular) lines should be compared with the gas-cooling rate due to dust.

It turns out that the two cooling rates are comparable in the relatively low density regime where the gas-cooling rate due to dust is dominated by the rate of transfer of thermal energy from the gas to the dust, *i.e.*

$$\begin{aligned} \mathcal{C}_{\text{g-d}} &= \frac{M}{\bar{m}} \left[\frac{8kT}{\pi \bar{m}} \right]^{1/2} \frac{3\rho Z_{\text{dust}}}{4r_{\text{dust}} \rho_{\text{dust}}} \\ &\times \left\{ 1 - \exp \left[\frac{-75\text{K}}{T} \right] \right\} \frac{k[T - T_{\text{dust}}]}{[\gamma - 1]}, \end{aligned} \quad (24)$$

rather than the rate at which the dust reradiates this energy (\mathcal{L}_{rad}). Additionally, at the low temperatures with which we are mainly concerned, we can simplify the analysis by setting the accommodation coefficient (the term in braces, $\{ \}$) to unity.

Putting

$$\frac{kT}{\bar{m}} = a^2 = \frac{GM}{JR},$$

the condition for line cooling to dominate over dust cooling becomes

$$R > R_{\text{crit}} \simeq \left[\frac{9\mathcal{J}^2 \hbar Z_{\text{dust}} I_{\text{CO}} [T - T_{\text{dust}}]}{32\mathcal{N}\mathcal{F}^2 G^2 r_{\text{dust}} \rho_{\text{dust}} [\gamma - 1] [T - T_0]} \right]^{1/3}$$

$$\times \left[\frac{m_{\text{CO}}}{\bar{m}} \right]^{1/6} \frac{c}{\bar{m}}. \quad (25)$$

With $\mathcal{J} = 2.4$, $Z_{\text{dust}} = 0.01$, $\mathcal{N} = 25$, $\mathcal{F} = 2$, $r_{\text{dust}} = 10^{-5}$ cm, $\rho_{\text{dust}} = 3$ g cm⁻³, $\gamma = 5/3$, and $\bar{m} = 4 \times 10^{-24}$ g, this reduces to

$$R > R_{\text{crit}} \simeq 0.3 \text{ pc} \left[\frac{T - T_{\text{dust}}}{T - T_0} \right]^{1/3}. \quad (26)$$

With a view to making R_{crit} as small as possible, we put $(T - T_0) \simeq 10$ K (e.g. $T_0 \simeq 3$ K and $T \simeq 13$ K). Then to reduce R_{crit} to 0.1 pc requires $(T - T_{\text{dust}}) < 0.3$ K, and to reduce it to 0.03 pc requires $(T - T_{\text{dust}}) < 0.01$ K. It would be an extraordinary coincidence if, *in a regime where gas-cooling by lines was dominant*, thermal balance were to deliver such a small value of $(T - T_{\text{dust}})$. We conclude that for fragments with $R \lesssim 0.1$ pc, gas-cooling is dominated by dust.

ACKNOWLEDGEMENTS

HMJB is supported by PPARC grant GR/K94157, and NF is supported by a PPARC studentship. We thank Cathie Clarke and Phil Myers for useful discussions.

REFERENCES

- Bate, M.R., Bonnell, I., Price, N.M., 1995, MNRAS, 277, 362
 Beichman, C.A., Myers, P.C., Emerson, J.P., Harris, S., Matthews, R.D., Benson, P.J., Jennings, R.E., 1986, ApJ, 307, 337
 Bodenheimer, P., 1978, ApJ, 224, 488
 Bodenheimer, P., Boss, A.P., 1981, MNRAS, 197, 477
 Bonnell, I., Bastien, P., 1993, ApJ, 406, 614
 Bonnell, I., Bate, M.R., 1994, MNRAS, 269, L45
 Boss, A.P., 1991, Nat, 351, 298
 Boss, A.P., 1993, ApJ, 410, 157
 Boss, A.P., Bodenheimer, P., 1979, ApJ, 234, 289
 Burkert, A., Bodenheimer, 1996, MNRAS, 280, 1190
 Chapman, S., Pongracic, H., Disney, M., Nelson, A., Turner, J., Whitworth, A., 1992, Nat, 359, 207
 Chièze, J.P., 1987, A&A, 171, 225
 Clark, F.O., 1987, A&A, 180, L1
 Hoyle, F., 1953, ApJ, 118, 513
 Kitsionas, S., Gladwin, P.P., Whitworth, A.P., 1998, in Star Formation with the Infrared Space Observatory, Joao Yun & Rene Liseau, eds., ASP Conf. Ser. 132, p. 434.
 Larson, R.B., 1972, MNRAS, 156, 437
 Larson, R.B., 1978, MNRAS, 184, 69
 Larson, R.B., 1995, MNRAS, 272, 213
 Low, C., Lynden-Bell, D., 1976, MNRAS, 176, 367
 Miyama, S.M., 1992, PASJ, 44, 193
 Miyama, S.M., Hayashi, C., Narita, S., 1984, ApJ, 279, 621
 Monaghan, J.J., 1994, ApJ, 420, 692
 Monaghan, J.J., Lattanzio, J.C., 1991, ApJ, 375, 177
 Myhill, E., Kaula, W.M., 1992, ApJ, 386, 578
 Nelson, R.P., Papaloizou, J.C.B., 1993, MNRAS, 265, 905
 Neufeld D.A., Lepp S., Melnick G.J., 1995, ApJSS, 100, 132
 Pringle, J.E., 1989, MNRAS, 239, 361
 Rees, M.J., 1976, MNRAS, 176, 483
 Scalzo, J.M., 1986, Fund. Cos. Phys., 11, 1
 Sigalotti, L., Klapp, J., 1994, MNRAS, 268, 625
 Silk, J., 1977, ApJ, 214, 152
 Simon, M., 1997, ApJ, 482, L81

Turner, J.A., Chapman, S.J., Bhattal, A.S., Disney, M.J., Pongracic, H.,
Whitworth, A.P., 1995, MNRAS, 277, 705
Whitworth, A.P., 1981, MNRAS, 195, 967
Whitworth, A.P., Clarke, C.J., 1997, MNRAS, 291, 578
Whitworth, A.P., Chapman, S.J., Bhattal, A.S., Disney, M.J., Pongracic, H.,
Turner, J.A., 1995, MNRAS, 277, 727